Electron Spin-Resonance (ESR) Studies of Adsorbate Dynamics on Single Crystal Surfaces: Possibilities and Limitations

U. J. Katter, H. Schlienz, M. Beckendorf, and H.-J. Freund

Lehrstuhl für Physikalische Chemie I, Ruhr-Universität Bochum, Universitätsstraße 150, 4630 Bochum 1

Adsorption / Electron Resonance / Interfaces / Spectroscopy / Surfaces

ESR is not one of the standard surface science tools because it is not inherently surface sensitive but rather probes the entire sample. However, ESR can be made into a surface science tool if we use paramagnetic adsorbates on thin nonmagnetic transition metal substrates or transition metal oxide films interacting with paramagnetic or nonmagnetic adsorbates. In contrast to NMR, ESR exhibits a sensitivity which allows one to detect monolayer and submonolayer coverages of spins ($>10^{12}$ spins). The experiments can be carried out either in ultrahigh vacuum (UHV) or under an ambient gas atmosphere. – ESR provides us with the unique opportunity to study adsorbate dynamics by studying line shape changes as a function of temperature. ESR is also sensitive to molecular orientation so that the orientation distribution of the molecular planes may be derived experimentally. Thus ESR allows us to derive information not easily accessible with other techniques. We describe the set up of a UHV/ESR experiment in which the ESR measurement may be combined with LEED/Auger and TDS experiments. Several types of results are discussed:

1. ESR of chemisorbed and physisorbed molecules on metal surfaces including angle dependent measurements.
2. ESR of molecules on oxide surfaces at submonolayers coverages.
3. We will touch on possible future experiments involving pulsed ESR techniques to study dynamics in the adsorbate for a wide variety of processes including rotation and diffusion.

Introduction

Magnetic Resonance, i.e. nuclear magnetic resonance, represents a class of spectroscopic methods which is most frequently applied in physics, chemistry, biology and, since the development of tomography, even in medicine [1–2]. In chemistry it is in fact the most important spectroscopic method supplying us with information on structure and dynamics of molecules in solution, molecular and non-molecular solids, polymers etc. [3]. The two- and threedimensional methods nowadays allow such investigations even for biological molecules. NMR-tomography has added a new dimension to it, i.e. spatial resolution [5]. In medicine it is now frequently applied as a diagnostic as well as a research tool to in vivo study specific functions of the metabolism [6, 7], for example. To study surface science of ideal systems, such as single crystal surfaces under UHV-conditions, NMR cannot be used at present because its limited sensitivity requires about 10^{18} nuclei in the sample. A surface only provides about 10^{15} sites and thus a molecular adsorbate in general only has a sample size of 10^{15} or smaller. Note, that in addition NMR is not inherently surface sensitive. Therefore this method is not used for ideal systems but for samples with large surface areas, powder samples or zeolites [8–10]. NMR already plays a very important and increasingly important role in the efforts to unravel reaction mechanisms in catalysis on real samples [11–15].

Another spectroscopic method which belongs to the same class is electron-spin-resonance (ESR) or electron-paramagnetic-resonance (EPR) spectroscopy [16–18]. It has the disadvantage to be exclusively applicable to systems

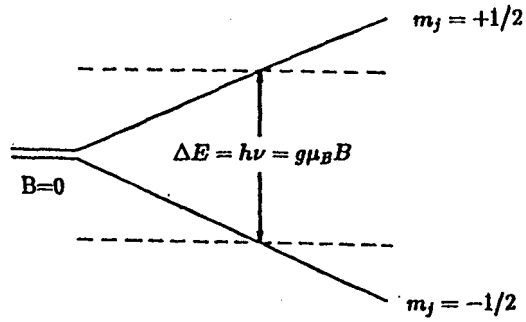

Fig. 1
Energy separation for the two energy levels of a free electron in a magnetic field

which contain unpaired electrons. However, its great advantage over NMR spectroscopy is its much higher sensitivity. The main reason is that the magnetic moment of the electron (Bohr magneton, μ_B) is by a factor of 2000 larger as compared with the nuclear magnetic moment. This quantity determines the energy separation between the levels (see Fig. 1) and thus the occupation difference which in turn determines the sensitivity of the experiment. The sensitivity of an ESR experiment is typically of the order of 10^{12} spins or even better. Therefore its sensitivity is high enough to allow detection of a monolayer or even a fraction of a monolayer of molecules with unpaired electrons on a surface of a single crystal with a surface area of 1 cm^2. This has been realized a long time ago. For example Göpel, Haul and coworkers in the late 60's designed a UHV-ESR-experiment to investigate semiconductor surfaces and ultrathin

  0005-9021/93/0303-000340 $ 10.00+.25/0

metal films on insulator substrates [19,20]. It was the general believe that such experiments on compact metallic single crystals are particularly difficult [21]. Therefore in the pioneering years of surface science where the main effort was concentrated on metallic surfaces, ESR, which in addition is like NMR not inherently surface sensitive, was abandonned. For real samples, however, ESR remained to be of great importance [21].

However, there have been some developments during the last years which have led us to reconsider ESR-spectroscopy as a possibly very powerful tool in the future to investigate structure *and* dynamics of adsorbed molecules on thin insulating films deposited onto a conducting, non magnetic, metallic substrate. In particular it is the aspect of dynamics of adsorbed molecules [22] that renders this method interesting because there is a lack of methods in the field of surface science to study these aspects. The recently observed developments addressed above mainly concern:

1. the first published successful ESR-experiment on NO_2 adsorbed on a rare gas covered Ag single crystal by K. Baberschke and his group [23–25].
2. the development of pulsed Fourier Transform-ESR by several groups, eg. J. H. Freed et al. [26–27], which has led to the first commercially available pulsed-FT-ESR spectrometers [18].

With these developments it appears possible in principle to collect, for example, twodimensional spectra and extract structural information. Also, spin-echo and other experiments shall allow to extract dynamical information covering a large time scale, namely between 10^{-3} s and 10^{-12} s. But even with continuous wave spectrometers it should be possible to perform temperature dependent measurements and observe line shape changes characteristic of freezing and unfreezing particular motions on well characterized surfaces.

ESR-spectroscopy has some further properties that are attractive with respect to applications in surface science.

Consider a gas phase at high pressure of a molecule which has no unpaired electrons, interacting with a non-magnetic substrate. Upon adsorption either the molecules or fragments or surface sites become paramagnetic then this can be detected if the concentration is high enough. Lunsford and his group have made some important contributions studying real samples to point out the importance of methyl-radicals in methane coupling [28]. Consider composed thin film systems where at the interface paramagnetic species are formed. It is possible to investigate the dynamics at the interface as a function of temperature. Consider polymer surfaces, which in situ have been spin labeled. By watching the temperature dependence of the spin label one may draw conclusions about the dynamics of the surface itself even if a non-paramagnetic gas phase is present.

This, of course, is not a complete list of possible applications of this technique, but it should be sufficient to demonstrate that a UHV-ESR-experiment is worthwhile, and that eventually ESR may turn into an in-situ method.

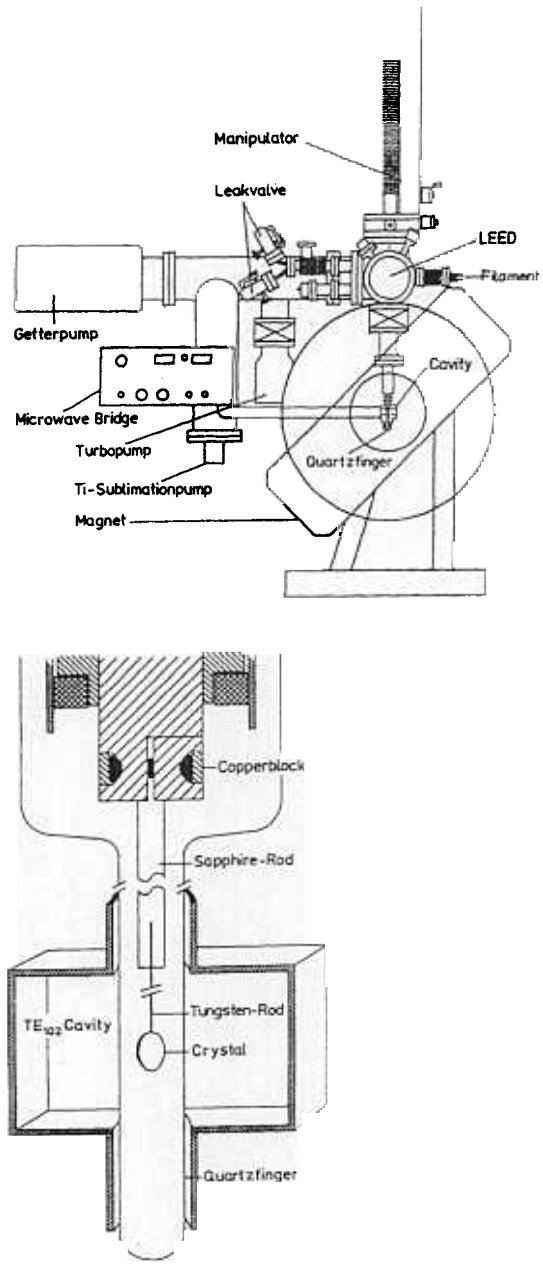

Fig. 2
a) Schematic diagram of a UHV-ESR spectrometer; b) Sample mount on the copper block of a He cryostat

We shall describe in the following our experimental setup, sample preparation and sample handling and then demonstrate the feasability of UHV-ESR-experiments on various samples, such as metal surfaces, metal-oxide surfaces and interfaces between molecular solids and metal surfaces.

Experimental Setup

a) The Apparatus

The experimental combined ultrahigh-vacuum-electron-spin-resonance apparatus is shown schematically in Fig. 2a. The bigger

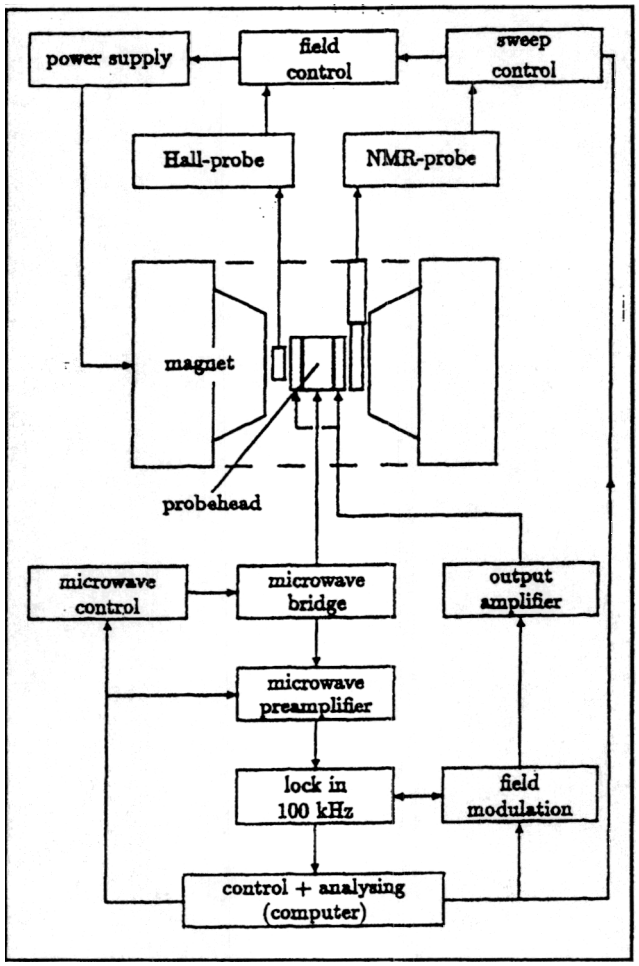

Fig. 3
Block diagram of the electronic setup

part of the UHV chamber is located above the magnet under measurement conditions. It is pumped by a set of turbo-, titanium-sublimation and iongetter pumps which create a base pressure of $1 \cdot 10^{-10}$ Torr. It is equipped with a back-view-LEED/Auger-unit (Omicron) and a quadrupol-mass-spectrometer to control the gas composition of the background and to perform TDS measurements. For the latter purposes a so called Feulner cup is mounted in front of the ionization chamber. To dose a gas to the surface a doser is available. Heating of the sample, which is attached by a special setup to the sample manipulator with a 600 mm z-translation shown in Fig. 2b, is done via a separately mounted filament. The sample may be positioned in front of the filament and it may be radiation heated or by electron impacts. The sample often is a circular thin (1 mm) nonmagnetic single crystal (e.g. Au(111) or NiAl(110)), which has a groove at the edge. This groove holds a tantalum wire loop. The ends of the loop are attached to a tungsten wire. The tungsten wire is pressed into a hole of a sapphire rod using a piece of metal foil. The sapphire rod electrically decouples the crystal from the copper block, which is the cooling stage of a self built He cryostat and at the same time guarantees good heat conductance to the crystal. With the long travel manipulator the sample may be moved to the upper part of the UHV chamber where both surfaces, i.e. both sides of the crystal, are cleaned and characterized with LEED and Auger spectroscopy. The crystal is then cooled to He temperatures. About 30 K may be reached as checked with rare gas adsorption. The sample is then exposed to molecules from the gas phase and the adsorbate is characterized with TDS. Once we know the preparation conditions a well defined adsorbate may be further characterized via ESR spectroscopy by moving the prepared surface into the microwave cavity. The top part of the chamber is fabricated from nonmagnetic V2A-steel. It ends with a valve which separates this part form a glass tube connected to the valve via a metal-glass connector. The glass tube has a wide bore near the valve and ends in a ESR suprasil tube of 9 mm inner diameter. The ESR tube sits within a microwave cavity (type TE 102) and it is connected with the clystron and the spectrometer electronics. This latter is a Bruker B-ER 420 ESR-spectrometer (magnet: 12") and it has been modified such that it can be computer controlled and the data may be stored in a IBM compatible PC. A block diagram of the electronic setup is shown in Fig. 3. The spectrum is taken by supplying a fixed radio frequency (9.5 GHz) and changing the magnetic field. A modulation frequency of 100 kHz is used routinely. It is ensured that the system does not saturate. The sensitivity of the setup has been determined in two ways: Firstly, the ultimate sensitivity of the cavity with suprasil finger (Q-factor: 3000) was measured by filling it with a given O_2 pressure and determining the disappearance of a particular O_2-line within the baseline noise. We find the sensitivity to be 10^{12} spins. Secondly, we introduced a small 4 mm · 7 mm polycrystalline copper foil which was treated with a benzene solution of diphenylpicrylhydrazyl (DPPH) of known concentration, and then the benzene was evaporated. Thus the copper foil was covered with a given number of spins, and we are in a position to determine the sensitivity of the setup including a metal sample to be about 10^{13} spins. This clearly shows that the presence of the metal piece in the cavity attenuates the sensitivity by about an order of magnitude but it shows at the same time that we still achieve submonolayer sensitivity.

b) Sample Preparation

So far we have investigated thin films of metal oxides with well ordered structure on top of a Au(111) and on top of a NiAl(110) single crystal surface with ESR spectroscopy. The Au(111) surface was completely covered with a NiO(111) surface according to a recipe described by Marre and Neddermeyer [29]. The NiAl(110) surface was completely covered with a γ-Al_2O_3(111) surface prepared according to a recipe by Jaeger et al [30].

NiO(111)/Au(111)

After heating (1000 K) and sputtering (2 μA680V 300 K) cycles the Auger spectrum of a Au(111) surface showed no surface contamination. The LEED pattern revealed the well known $(22 \pm 1) \cdot \sqrt{3}$ reconstruction described elsewhere [31]. Onto the such prepared reconstructed Au(111) surface Ni is evaporated and subsequently oxidized in an oxygen atmosphere. This procedure leads to a well ordered NiO(111) film which exhibits a thickness such that the Auger spectrum revealed no metallic Au. The NiO(111) layer is about 10 ML thick. A similar NiO(111) surface can be grown on top of a metallic Ni(111) surface [32]. Such a NiO(111) surface has been characterized with respect to several surface spectroscopic methods, e.g. XPS, HREELS, ISS, TDS. The system NiO(111)/Ni(111) has been studied towards adsorption of several molecules, e.g. CO, NO, CO_2, H_2O and NO_2 and the results gained in these studies [32] can be transferred to NiO(111)/Au(111).

γ-Al_2O_3(111)/NiAl(110)

When a clean nonmagnetic NiAl(110) surface, which is characterized by a sharp LEED pattern, is oxidized through various cycles, the system exhibits a characteristic LEED pattern with a large unit cell in real space. This oxide layer has been extensively studied with various electron spectroscopic methods and scanning tunneling microscopy [33] and adsorption of several molecules has been investigated [34].

We have studied with ESR spectroscopy adsorption of NO_2 on Au(111), NiAl(110), NiO(111)/Au(111) and on γ-Al_2O_3(111)/

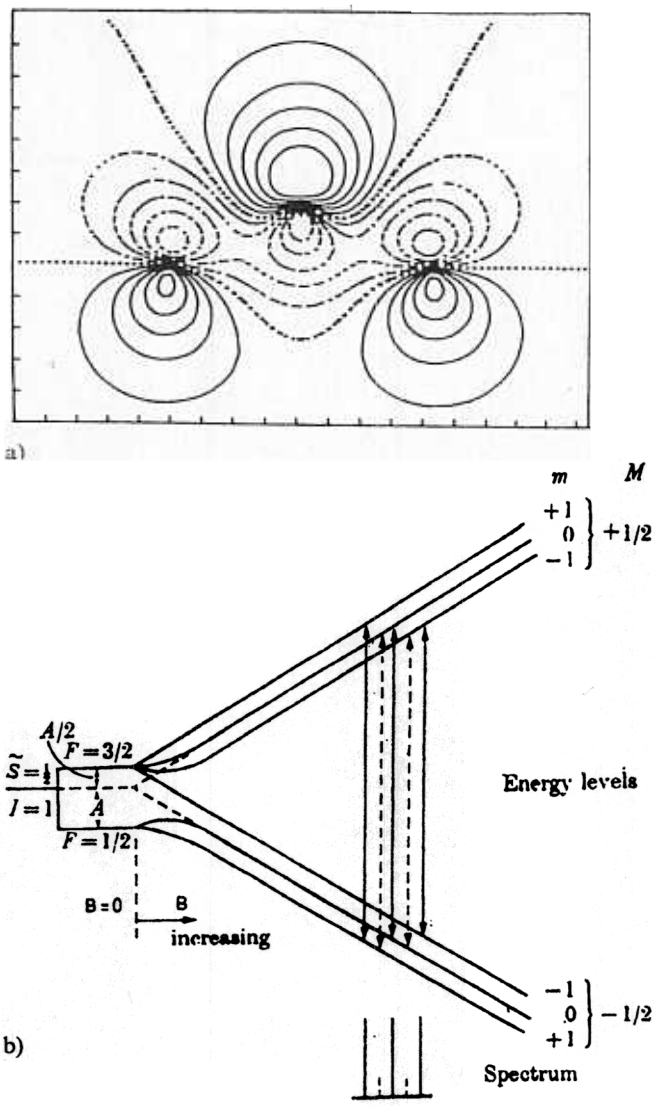

Fig. 4
a) Electron density contour plot for the $6a_1$ orbital of free NO_2 [35]; b) Level splitting diagram for a system with $S = 1/2$ and $I = 1$ without and with increasing magnetic field. The weak transitions where the nuclear spin is changed in the transition and which are not considered here are indicated as broken lines

NiAl(110). The gas was taken from a lecture bottle with 99.5% purity, and it was cleaned by removing water via well known procedures. The cleaned NO_2 was dosed either from the background or from a doser close to the sample surface.

Results and Discussion

The following discussion will proceed by first considering adsorption of NO_2 on a clean metal surface. We shall show that a monolayer of NO_2 on Au(111) does not exhibit an ESR spectrum and the reasons for this behaviour will be evaluated. In a second step adsorption of NO_2 on thin oxide films is studied. Before we start with the discussion of the adsorbates, however, we shall quickly address the ESR spectrum of free gaseous NO_2.

NO_2

The NO_2 molecule has a nonlinear geometry with a N–O bond length of 1.197Å and a O–N–O angle of 134.15° and belongs to the point group C_{2v}. The ground state of the molecule has the term symbol $^2A_1$, where the unpaired electron resides in a $6a_1$ molecular orbital which is shown in Fig. 4a [35]. Thus the paramagnetism of the NO_2 molecule is determined by $S = 1/2$ and $L = 0$, and we expect a g-value close to that of the free electron, i.e. $g = 2$. An important factor for ESR spectra is the hyperfine interaction (A) of the electron spin with the nuclear spin ($I = 1$) of the ^{14}N atom, while the oxygen atoms ^{16}O have vanishing nuclear spin ($I = 0$) and thus do not couple. Without a magnetic field the levels are split in two components ($F = 1/2$, $F = 3/2$), but with a finite magnetic field these levels split into six sublevels with $m_J = (0, 1, -1)$ and $M = (1/2, -1/2)$ as shown in Fig. 4b. If the molecules were fixed in space, the selection rule for dipole transitions $\Delta m_J = 0$, $\Delta M = 1$ would lead to a spectrum consisting of three equally intense lines and an energy separation dictated by the hyperfine interaction, which is a local property at the nitrogen center. However, there is not only coupling between electron angular momentum and nuclear angular momentum but also coupling to molecular rotations which leads to the appearance of a large manifold of lines. The gas phase NO_2 spectrum has been discussed and assigned in detail by Burch et al. [36] for example.

NO_2/Au(111); NO_2/NiAl(110)

The system NO_2/Au(111) was chosen because it has been thoroughly studied with TPD and HREELS by Koel and his group [37]. Unlike NO_2 adsorbates on other coin metals where the chemistry at the surface is not well known, and it is very likely that rather complex reactions take place at the surface, the system NO_2/Au(111) exhibits a very clean and simple adsorption behaviour as revealed by the TPD data shown in Fig. 5a. In complete agreement with the work by Bartram and Koel [37] we observe a desorption peak for the monolayer at $T = 230$ K well separated from a multilayer peak at $T = 150$ K. Therefore by setting the surface temperature appropriately we can study the monolayer or the multilayer separately. Bartram and Koel [37] have shown via HREELS that in the monolayer regime the NO_2 adsorbs molecularly and there is no sign of any reaction product. A detailed analysis of the HREELS spectrum reveals that the NO_2 is bound in a surface site of C_{2v} symmetry with its molecular plane perpendicularly oriented towards the surface plane. It is likely from the work of Bartram and Koel [37] that the molecule is bound with both oxygen atoms as opposed to the nitrogen atom towards the surface. Whether the bonding mode is bidentate to a single metal atom or to two metal atoms is not clear at present. In any case the electron spin which couples to the ^{14}N nuclear spin will provide information from an ESR experiment about the involvement of the nitrogen atom in the chemical bond to the substrate. In Fig. 5b the ESR spectra corresponding to the TPD spectra (Fig. 5a) are shown.

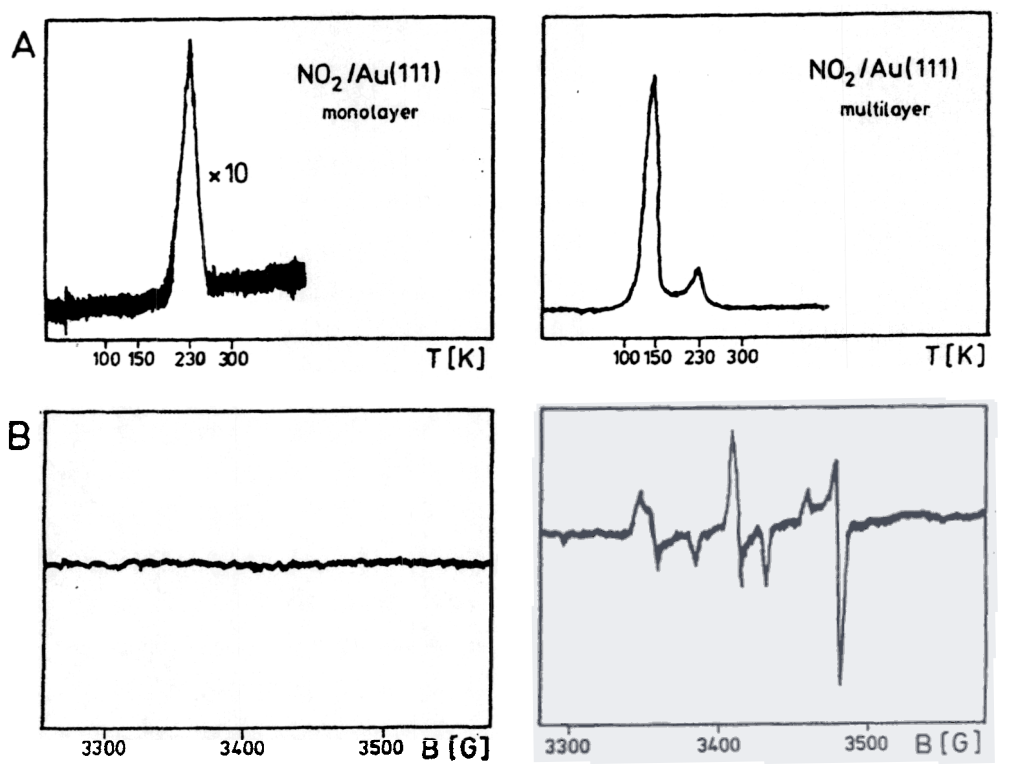

Fig. 5
Thermal desorption (TPD) and ESR spectra ($T = 35$ K) of NO_2/Au(111); a) TPD signal for a monolayer NO_2 coverage (left panel); TPD signal for a multilayer coverage (right panel); b) ESR spectrum for a monolayer NO_2 coverage (left panel); ESR spectrum of a multilayer coverage (right panel)

Clearly for the multilayer we observe a rather well resolved solid state spectrum of the NO_2 molecular solid which we shall analyse in more detail further down. On the other hand the monolayer shows no ESR signals above the background. This latter result is not completely unexpected because Baberschke and his group has performed a similar experiment on a Ag surface where there was no ESR spectrum detected. However, since the chemistry of NO_2 on Ag is not well documented, the present result is more clear cut. The explanation given by Baberschke et al. was [23–25] – and we agree with this interpretation – that the interaction between the electrons at the Fermi energy of the metal substrate and the electron spin on the molecule is so strong that the average residence time of the electron spin on the molecule is strongly reduced. This effect, which is called Korringa-correlation [38], leads to a strong increase of the line width such that the spectrum disappears in the background noise. The lines are recovered if the molecules are isolated from the metal surface by an inert gas layer as was also shown by Baberschke and his group [23–25]. Based on this observation we use a thin oxide layer as the surface spacer as we shall discuss in the following sections. Before we turn to the oxide surfaces, however, we would like to come back to a more detailed discussion of the NO_2 multilayer on the Au(111) surface. We may refer to a very detailed discussion by Schaafsma, Velde and Kommandeur in 1967 [39–41], who worked out the ESR spectrum of NO_2 in a polycrystalline matrix of N_2O_4. Schaafsma et al. [39–41] reported that a condensed N_2O_4 layer as prepared exhibits no ESR spectrum. Only after photochemical initiation did these authors find NO_2 molecules embedded in a N_2O_4 matrix. This is precisely the nature of the multilayer system. Photochemical initiation was not necessary in our preparation.

Briefly, Fig. 6 schematically shows the way a solid state NO_2 spectrum with randomly oriented molecular planes develops from the spectrum of an isolated molecule. If all NO_2 molecules were oriented with their molecular plane the same way with respect to the magnetic field, one would observe a spectrum sonsisting of a single triplet. Depending on the orientation of the main axis of inertia towards the magnetic field, there are three different g-values ($g_{a,b,c}$) and three different hyperfine coupling constants ($A_{a,b,c}$) which represent the three components of the g and A tensors after diagonalization. Thus there are three types of triplets which may be observed if there are differently oriented molecules in a sample and their orientations were fixed. They are represented by the diagrams b)–d) in Fig. 6. They may be sorted in the three groups of m_j-values, i.e. -1, 0, 1, indicated in diagram a). In a real sample there are many possibly random orientations allowed of the main axis relative to the magnetic field. Therefore, one does not only observe the three extreme values per m_j-value but also all intermediate values. If all contributing lines to the three m_j-values are assumed to be δ-functions, the spectrum in diagram e) results. For finite line widths the spectrum is modified as in

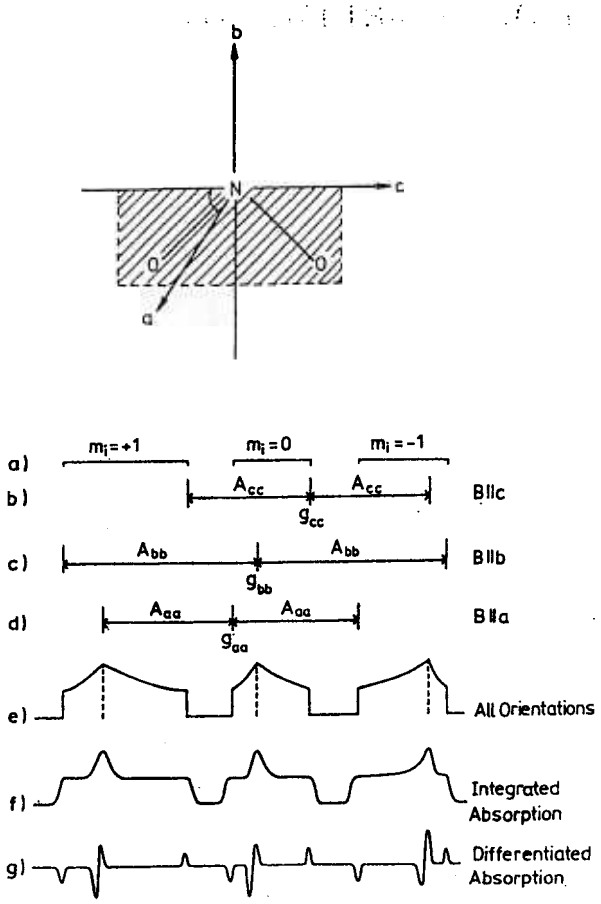

Fig. 6
Schematic diagram to indicate the development of a solid state ESR spectrum of molecules with fixed, threedimensionally random orientations [39]. The chosen coordinate system and the nomenclature for the principal axis is indicated

Table I

system	g-tensor			A-tensor [G]			ref.
gasphase							
NO_2-gas	2.00618	2.00199	1.99102	45.60	66.02	45.20	[42]
matrix isolation							
N_2O_4	2.0054	2.0015	1.9913	50.2	68.3	49.6	[38]
N_2O_4	2.0065	2.0029	1.9960	50.2	68.3	49.6	[43]
Argon(4K)	2.0051	2.0024	1.9914	50.6	63.1	45.4	[44]
Neon(4K)	2.0054	2.0026	1.9919	50.9	63.5	45.9	[44]
adsorption							
Zeolite(Na-X)	2.0043	2.0015	1.9922	51.1	67.5	49.2	[45]
Zeolite(Ca-X)	2.0051	2.0017	1.9921	51	67.6	47.8	[45]
Zeolite(Na-Z)	2.0051	2.0017	1.9913	49.9	65.5	45.9	[22]
ZnO	2.007	2.003	1.994	52.0	64.8	47.3	[46]
MgO	2.005	2.002	1.9915	52.7	67.5	49.1	[47]
Xenon(20K)	2.0045	2.002	1.9915	48.5	64	44.5	[25]
Argon(20K)	2.0055	2.002	1.9915	49	64	45	[25]
Krypton(20K)	2.0055	2.001	1.9915	49	64	45	[25]
NO_2/Au(111)	2.0050	2.0010	1.9912	49.61	66.66	47.31	this work
NO_2/Al_2O_3/NiAl	2.0055	2.0019	1.9920	51.53	66.17	50.08	this work

diagram f). Since the ESR spectra are generally reported in the differentiated form, diagram g) shows the differentiated diagram f). This explains the principle features observed for the NO_2 spectrum in the multilayer (Fig. 5b).

If we compare an experimental spectrum with a computer simulated one under the assumption of random orien-

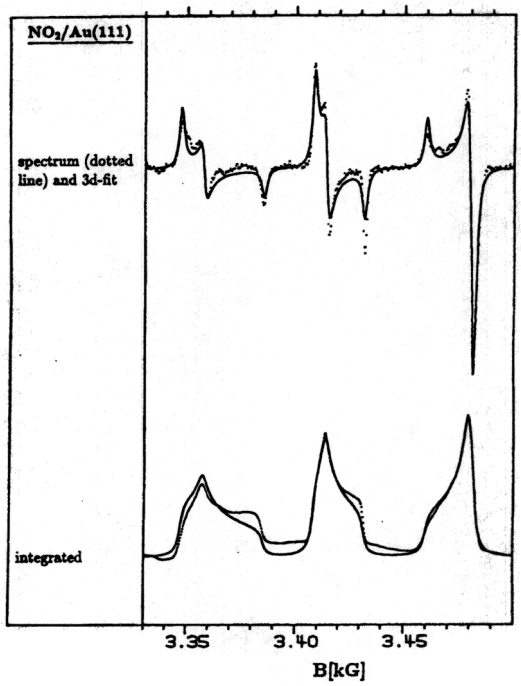

Fig. 7
ESR spectrum of a multilayer NO_2 on Au(111) taken from Fig. 5b fitted by a computer simulated threedimensional random distribution. Upper panel: differentiated spectrum; Lower panel: integrated spectrum

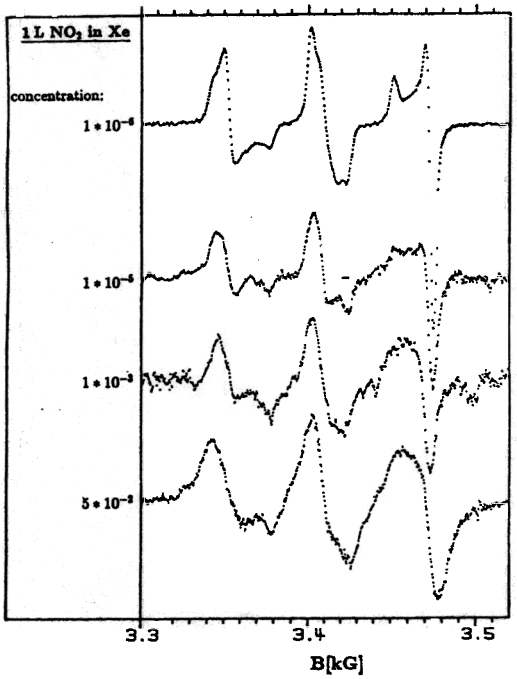

Fig. 8
ESR spectra taken of a cocondensed film of Xe and NO_2 ($T = 35$ K). 1 L NO_2 was dosed within a background pressure of Xe. The crudely estimated concentrations are indicated with the spectra

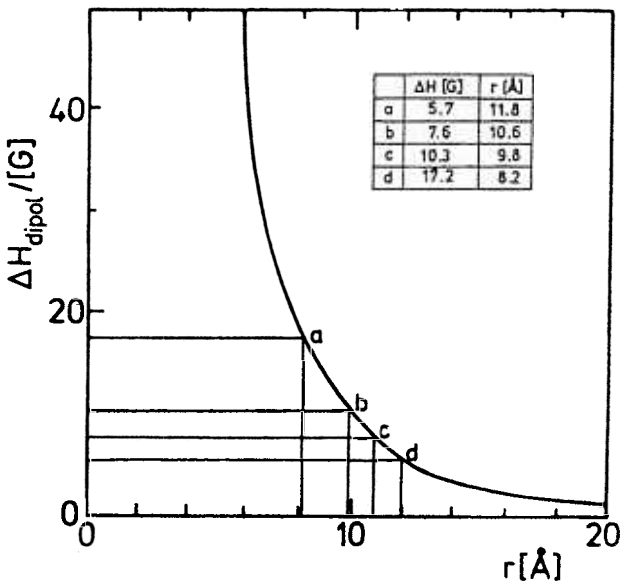

Fig. 9
Plot of the intermolecular dipole-dipole interaction as a function of distance [48]. The intermolecular distances deduced from the measured linewidths (Fig. 8) are given in the inset

tation as done in Fig. 7, we see rather good agreement. Both, the differentiated as well as the integrated spectra are shown. The fit delivers g and A values and a line width for an individual contributing orientation. The values are collected in Table I where they can be compared with all other values reported in this study including literature values. The g value is close to the free electron value and the A values are typical for undistorted NO_2. The line width is in line with non interacting NO_2 molecules. The effect of increasing dipole-dipole interaction between coadsorbed molecules on the line width can be seen from Fig. 8, where NO_2 has been cocondensed with varying amounts of Xenon such that the concentration decreases by four orders of magnitude. This translates into a decrease in the intermolecular distance. It is quite obvious that the line width increases considerably, while the spectrum can still be fitted by a threedimensional random distribution of the NO_2 molecules. We observe an increase by a factor of 3 in the line width from 5.7 G to 17.2 G. In Fig. 9 the line width as observed in Fig. 8 are placed in a plot taken from Kittel and Abrahams [48] on the connection between line width and intermolecular distance $\Delta H_{dip} \sim 1/r^3$. From this we derive the average intermolecular distance in our sample. It means that the ESR spectrum at the bottom respresents an intermolecular distance of 8.2 Å which may be compared with the NO_2 van der Waals radius of about 4 Å. The line width of the ESR spectrum at the top of Fig. 8 suggests, if analysed via Fig. 9, that the intermolecular distance has increased by 50%. This is an important conclusion for future adsorbate studies. Note, however, that there may be other contributions to the line width, such as the above mentioned Korringa coupling [38] and others that we have not discussed in this paper [49].

An important information one might want to extract from spectroscopic data, is the orientation of adsorbed molecules. Usually this is done by angle dependent measurements. The angle dependent capabilities of the ESR experiment, where the angle between magnetic field and surface normal can be varied by turning the sample within the cavity can be demonstrated. Fig. 10a shows a set of angle dependent spectra of NO_2 on Au(111) taken in a rectangular cavity. There are no angle dependent line shape changes observed in this case, in line with the assumption that the distribution is threedimensionally random in the present data. The overall decrease of intensity is caused by the particular field distribution in the cavity. The angular dependence can, however, be used to analyse more complex systems where there are oriented species present. Fig. 10b shows a series of angle dependent spectra taken for NO_2 on NiAl(110). NO_2 reacts with NiAl(110) leading to several N containing species with unpaired electrons on the eventually oxidized surface. We do not want to present a detailed analysis of the adsorbate system but rather indicate how the angular dependence allows identification of these species. At 0° degrees we find a spectrum which resembles a threedimensionally random NO_2 adsorbate. At 90° there is an extra triplet overlapping the spectrum of a randomly oriented NO_2 distribution, indicating that there is a chemically different NO_2 species present on the surface which is oriented with it molecular plane relative to the surface plane.

NO_2/γ-Al_2O_3(111)/NiAl(110)

In our group there has recently been increasing interest to understand in more detail adsorption of molecules on oxide surfaces in order to complement our knowledge on metal surfaces. It is our goal to apply electron spectroscopic methods, and we have therefore tried to avoid the study of bulk, insulating oxide single crystals. Instead, we have resorted to thin, well ordered oxide films which can be grown in situ on metal surfaces. γ-Al_2O_3(111) may be grown as a 5Å thick film on the surface of an alloy single crystal, i.e. NiAl(110) [34]. We have studied physisorption of a series of simple molecules on the oxide surface. We know that NO_2 on the other hand more strongly interacts with the γ-Al_2O_3(111) film. It was therefore near at hand to study the interaction in this system with ESR spectroscopy. In addition we wanted to elucidate the possibilities of employing ESR spectroscopy as a tool to study the dynamics of adsorbed molecules.

Fig. 11 shows a set of ESR spectra together with the corresponding TPD spectra starting with 0.2 L up to an exposure of 2 L. We can follow the development of the spectra starting with rather poor signal to noise below 1 L. At 2 L the signal to noise has improved and the spectrum is characterized by a rather large line width. It is not clear, without further proof, what causes the large line width, but we believe at present that it is a consequence of the strong

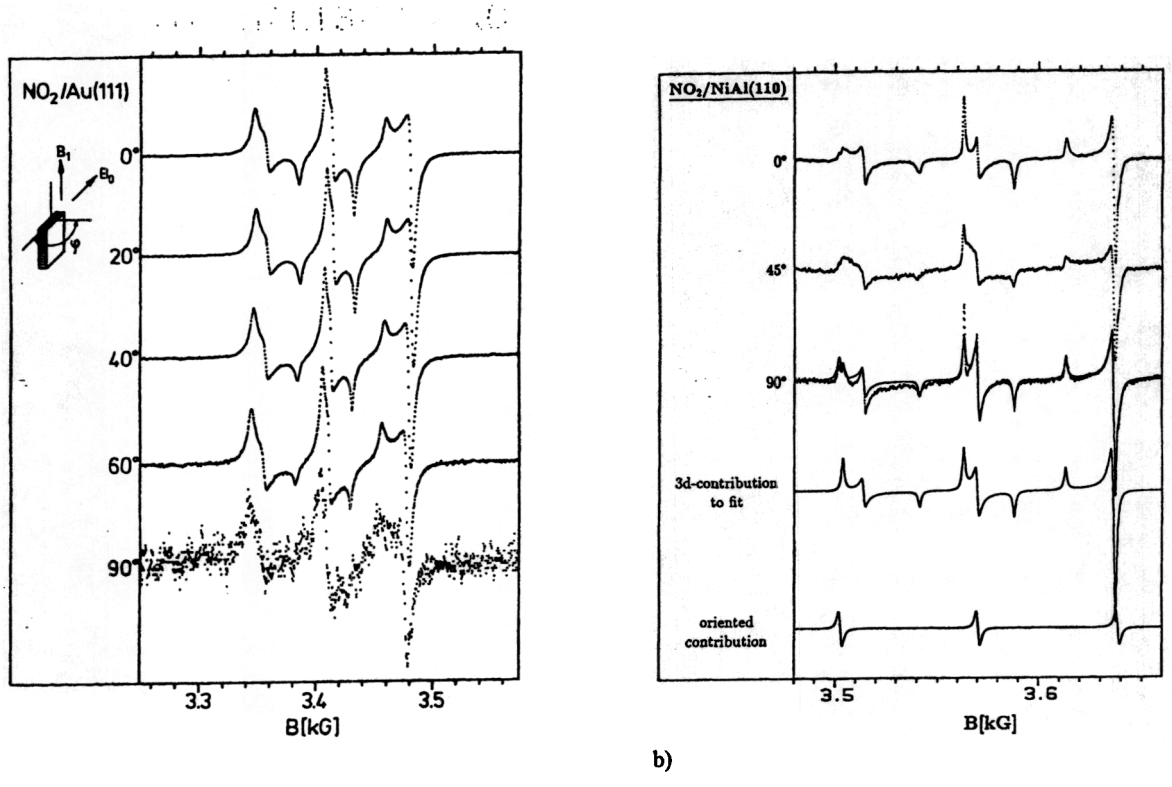

Fig. 10
a) ESR spectra of a multilayer of NO_2 on Au(111) at $T = 35$ K as a function of the angle between the surface and the magnetic field (see inset); b) Angle dependent ESR spectra of NO_2 reacted with a NiAl(110) surface at low temperature. The decomposition in a threedimensional random distribution and a triplet is shown

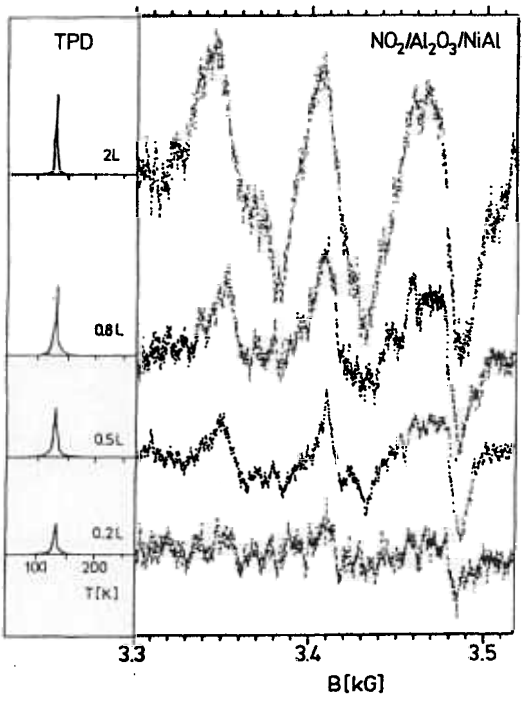

Fig. 11
ESR spectra as a function of coverage of NO_2 on $Al_2O_3(111)$/NiAl(110). For each ESR spectrum the TPD spectrum is also shown. The spectra were taken at $T = 35$ K

intermolecular interaction. If the large line widths are indicative of strong intermolecular interaction, then the data suggest that the great majority of molecules do not dimerize because N_2O_4 would not contribute to the ESR spectrum but represent a rather inert matrix (see Fig. 8) for the remaining NO_2 molecules. This in turn would lead to much smaller line widths. Note that at intermediate coverages the spectrum reveals extra structure in particular at 3.46 kG. Indeed, if we dose more and more NO_2 on the surface, the lines eventually become sharper because the inert N_2O_4 matrix forms. Fig. 12 shows the differentiated and integrated spectrum recorded for a dose of 100 L. The fit to the data is a combination of a threedimensional random and a twodimensional distribution. A single threedimensional distribution would result in unacceptable deviations and even the combined fit shows significant deviations. Below the combined fit are shown the two composing distributions seperately. The twodimensional distribution refers to NO_2 molecules which are oriented with the molecular plane perpendicular to the surface plane. For comparison a distribution of molecules with their axis oriented parallel to the surface plane are shown. There is a clear differentiation between the two orientations possible via the analysis of the spectra.

We attribute the existence of a superposition of a twodimensional and a threedimensional distribution of NO_2 molecules to the coexistence of a physisorbed multilayer on top of a monolayer of molecules in direct contact with the $Al_2O_3(111)$ surface. The persisting deviations, however, can-

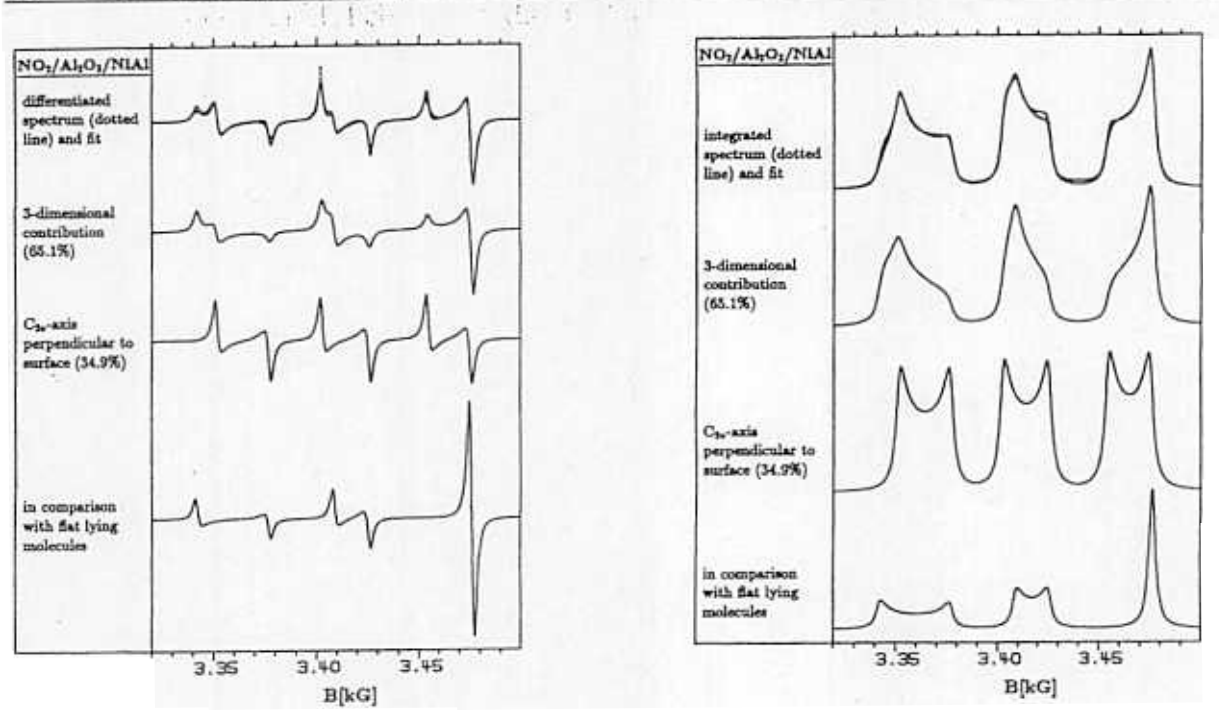

Fig. 12
ESR spectrum at $T = 35$ K of a thick NO_2 layer (100 L) on Al_2O_3(111)/NiAl(110) fit by a combination of a threedimensional random and a twodimensional (molecular plane perpendicular to surface) distribution. The decomposition is shown. For comparison a twodimensional distribution with flat lying molecules is included. The two panels show the differentiated as well as the integrated form of the spectra

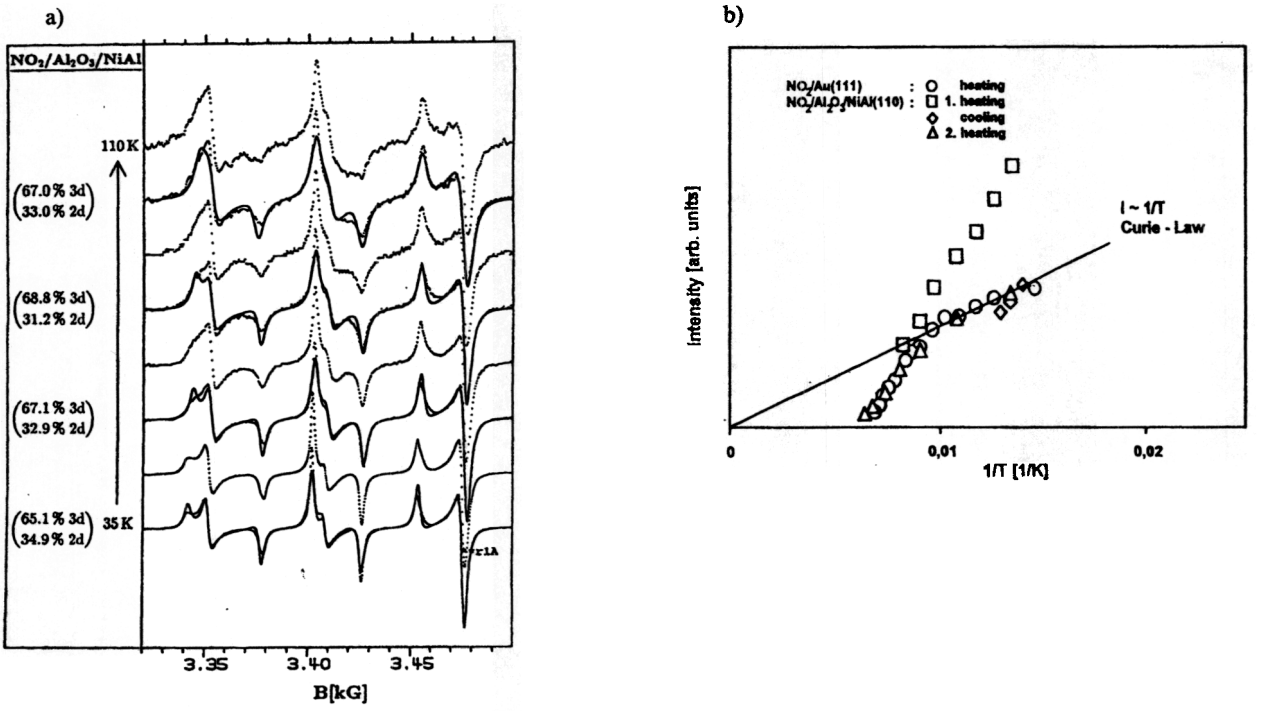

Fig. 13
a) Series of ESR spectra as a function of temperature. For some spectra a fit similar to the one shown in Fig. 12 is included. The relative contributions of the threedimensional and twodimensional distributions are indicated; b) Temperature dependence of the integrated intensity of the ESR spectra of Fig. 13a. The temperature dependence expected from a Curie law is indicated by the solid line

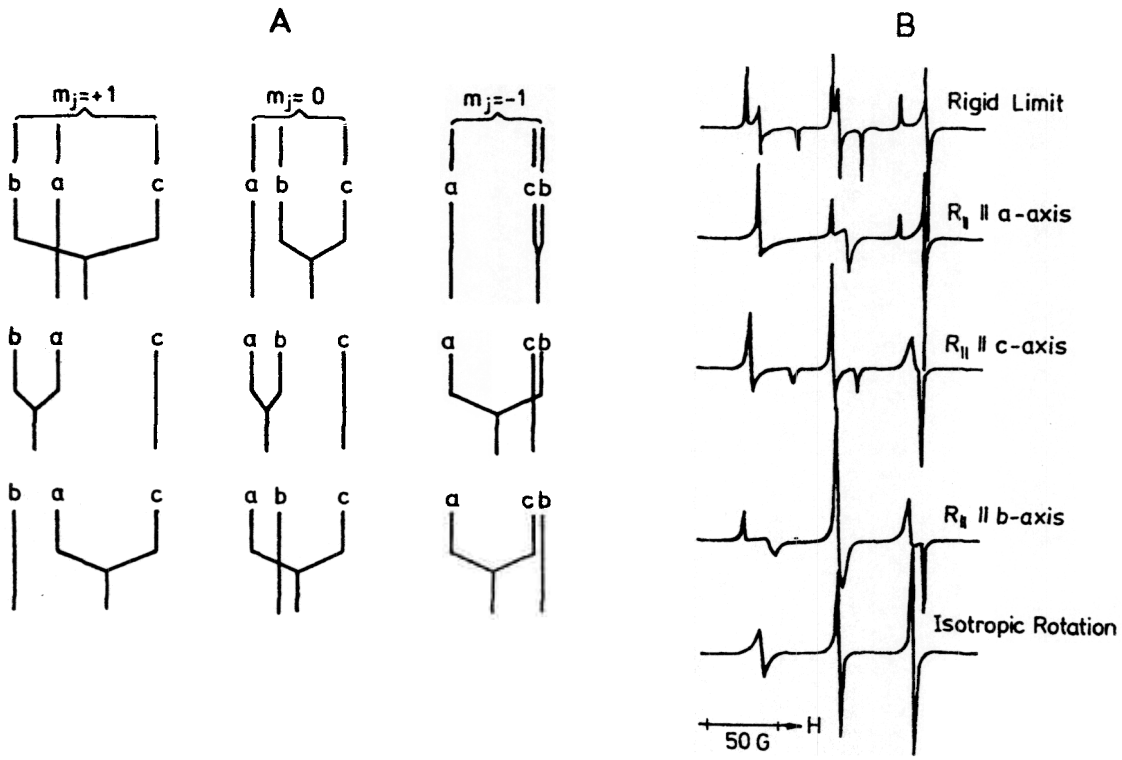

Fig. 14
Schematic diagram showing the influence of molecular motion onto the line shape of ESR spectra; a) Extreme values for the absorption lines corresponding to the various A tensor components for a threedimensionally fixed random orientation (top) in comparison to the three cases when rotation about the principal axis becomes fast [39–41]; b) Computer simulations corresponding to the bar diagrams in Fig. 14a. For comparison the case of isotropic rotation is included [22]

not be explained by static distributions. We suspect that they are a consequence of molecular motion of the molecules in the system. Further computer simulations to incorporate this aspect are in progress.

What happens to the adsorbate if we change the surface temperature? Fig. 13a shows a temperature series starting at low temperature (bottom) moving to high temperature (top) where the spectra have been normalized to the same maximum intensity. The change of the absolute intensities is given in Fig. 13b. The intensities are plotted versus the inverse temperature because we expect a Curie-type (straight line) behaviour for the resonance intensity of the paramagnetic NO_2. The NO_2 overlayer on Al_2O_3/NiAl(110) exhibits a temperature dependence different from the Curie behaviour. The signal decrease (□) is much faster upon heating the layer to a temperature close to desorption. But if the process is stopped at this point and the sample is cooled down again (◇) the data follow the straight line. The reason for this observation is that dimerization is taking place by allowing the NO_2 molecules in the N_2O_4 matrix or in the monolayer to move thus effectively removing the molecules from the spectrum. Upon recooling the adsorbate the expected $1/T$ behaviour is found. If we perform the same experiment again the datapoints (Δ) follow the Curie behaviour when heated, and as soon as we reach the desorption temperature molecules are removed from the surface as indicated by the faster decrease of the signal intensity at 0.01 K^{-1} inverse temperature. The latter behaviour is also found for a NO_2 physisorbate on Au(111) (o). As pointed out above, the distributions contain two contributors, namely a threedimensional (3d) and a twodimensional (2d) component. Fig. 13a also shows simulations of the data overlaying the experimental data and gives the relative 3d and 2d contributions for each spectrum. There is no significant change in the relative contributions as the temperature increases but we observe a slight change in line width. This could be due to translational motion of the NO_2 monomers in the physisorbed N_2O_4 film. The interaction between the excited monomers and the surrounding molecules decreases the lifetime of the excited states and this leads to an increase of the line widths. Although the fit between experimental data and computer simulation is rather good there are significant deviations in parts of the spectrum. It is quite likely that these deviations are due to the lack of taking molecular motion into account. The incorporation of molecular dynamics into the simulation is difficult in particular if the time scale of the motion is comparable to the time scale of the ESR experiment [27]. In the limiting case that the motion is fast, the situation is rather simple as scetched in Fig. 14a [40]. Results of calculations by Freed et al. for this case are shown in Fig. 14b [22]. For the three m_j components the extreme values according to the three principle axis, a, b, c (see Fig. 6) are given. In the topmost diagram the spectrum for the threedimensional

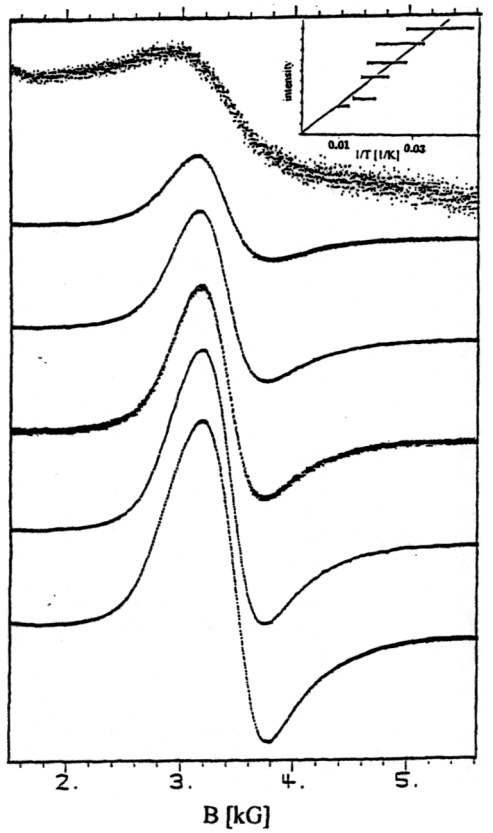

Fig. 15
Temperature dependence of the ferromagnetic Ni resonance as measured for the system NiO(111)/Au(111). The intensity is plotted versus $1/T$ in the inset

fixed random distribution is shown as discussed in connection with Fig. 6. In the other diagrams fast rotation about the principle axis *a*, *b*, *c*, respectively, has been assumed. If fast rotation is carried out about axis *a* the distribution about axis *b* and *c* is averaged out and collapses into one line. This phenomenon is called motional narrowing. Corresponding situations are found if fast rotation about the other two axis is carried out. If we included this aspect in the analysis of the spectra we believe that fits are created improving over the combination of a static twodimensional and a static threedimensional distribution.

NO_2/NiO(111)/Au(111)

NiO(111) is another oxide surface we have started to study with ESR spectroscopy recently. When Ni is evaporated onto a Au(111) substrate and oxidized with oxygen to form the epitaxial NiO(111) overlayer, the NiO(111) film, although it covers the surface of the Au(111) crystal perfectly, contains a rather small number of Ni particles as revealed by ESR spectroscopy. Fig. 15 shows ESR spectra taken of a clean NiO(111) surface as a function of temperature. A resonance typically observed for small Ni particles on glass substrates [19,20] is found in the present case. The position is consistent with the ferromagnetic resonance of Ni as well as is the temperature dependence of the resonance intensity as shown in the inset of Fig. 15. The concentration of the Ni particles is small so that they do not interfer with adsorption of gases.

NO_2 adsorption has been tried. It is interesting to note that contrary to γ-Al_2O_3(111)/NiAl(110) which is sensitive to NO_2, NiO(111) appears to be inert in the sense that NO_2 adsorption does not irreversible change the structure of the substrate. The LEED pattern remains unchanged upon adsorption, indicating that there is no ordered layer of NO_2 on the surface and that there is no effect on the structure of the substrate. The adsorption behaviour is simple. There is a monolayer and a multilayer regime. In the case of NO_2/NiO(111) we have checked the NO_2 coverage of the NiO(111) surface with XPS [32]. (The measurements were done for the system NiO(111)/Ni(111)). Fig. 16 shows a set of XPS N1s spectra where we can separate the mono- and the multilayer by the binding energy difference. The saturating N1s peak at 403.5 eV is due to the monolayer of NO_2 while the peak at 405.5 eV is due to the N_2O_4 in the multilayer. The ESR spectrum of a multilayer is shown in Fig. 17. It is similar to the spectrum of NO_2 on γ-Al_2O_3(111) indicating rather strong dipole-dipole coupling via the large line width of the signal. At present we are trying to fit the spectra including molecular motion by computer simulations.

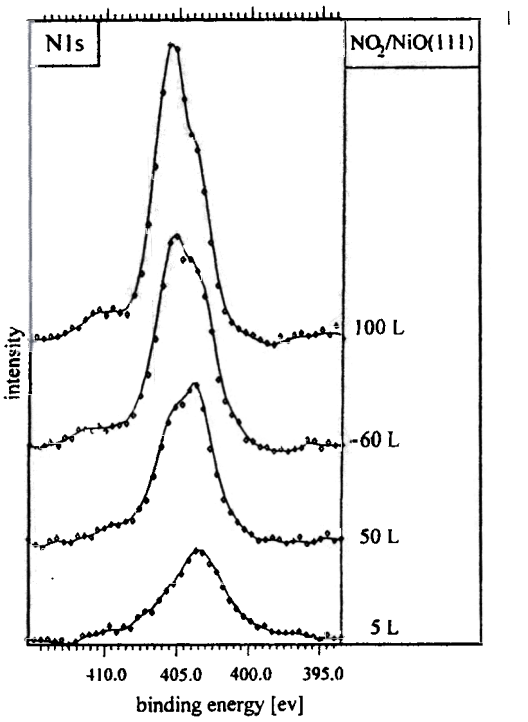

Fig. 16
XPS N1s-spectra of NO_2/NiO(111)/Ni(111) [32] as a function of coverage

Summary and Perspective

We have shown that ESR spectroscopic investigations can be carried out on single crystal surfaces under UHV con-

ditions. NO_2 on metallic substrates, such as Au(111) leads to a vanishing ESR spectrum due to the large line width created by the interaction of the electron spin on NO_2 with the electrons at the Fermi energy of the metal substrate in good agreement with Baberschke et al [3–5]. On metal oxide surfaces, on the other hand, which we prepare by epitaxially growing a single crystal oxide layer on top of a metal (Au, NiAl) substrate, ESR signals in the monolayer and in the multilayer regime can be observed. The line widths, which are dominated by dipole-dipole interactions, change characteristically as the intermolecular interaction increases. From the spectra we can also extract the dimensionality of the NO_2 adsorbates through line profile fittings. Angle dependent measurements where the angle between the sample surface and the magnetic field is varied allow the determination of the orientation of the molecular NO_2 plane on the substrate surface. This is not only so for the uncovered monolayer but also if the monolayer is covered by an rather thick physisorption layer. ESR spectroscopy is therefore a potential candidate to look at burried interfaces if these contain paramagnetic centres. The investigation of temperature dependent spectra indicates characteristic changes of the line shapes as a function of temperature which can be related to the dynamics in the adsorbate systems.

Of course, thermally activated processes like desorption and chemical reactions in the adsorbate layer can be investigated as was illustrated by looking at the recombination reaction

$$2\,NO_2 \rightleftarrows N_2O_4$$

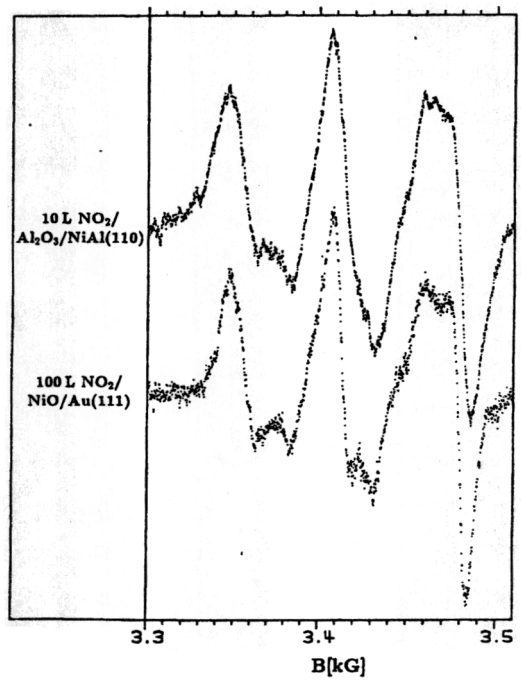

Fig. 17
ESR spectrum of NO_2/NiO(111)/Au(111) in comparison with NO_2/Al_2O_3(111)/NiAl(110)

The sensitivity of the experiment to magnetic centers also allows interesting in situ studies of film growth. The ferromagnetic resonance and its characteristic temperature dependence have been observed for Ni clusters in a NiO(111) matrix but a systematic study has to follow up.

So far we have only briefly adressed the question of molecular motion in the adsorbate. ESR, we think, can be a very powerful tool to study such phenomena in the future if the spectra can be recorded with sufficient signal to noise. If it is possible to apply the recently developed pulsed Fourier-transform ESR methods including classical spin echo detection and twodimensional techniques, then ESR may give us important novel information on dynamic processes on surfaces. This is not to say that ESR spectroscopy could eliminate other classical surface science methods. On the contrary, it will be an additional, complementary tool for the study of particular aspects of adsorption which are hard to achieve with other methods.

The particular aspect that makes it worthwhile is that ESR can be applied to single crystal surfaces as well as to polycrystalline surfaces and real catalysts even under non UHV conditions. It is hoped that through the application of this method we can help in the future to bridge the gap from surface science to catalysis.

We are grateful to the Deutsche Forschungsgemeinschaft and the Ministerium für Wissenschaft und Forschung des Landes Nordrhein-Westfalen for financial support. H.-J. Freund thanks the Fonds der Chemischen Industrie.

References

[1] R. R. Ernst, G. Bodenhausen, and A. Wokaun, "Principles of Nuclear Magnetic Resonance in One and Two Dimensions", Clarendon Press, Oxford 1986.
[2] H. Friebolin, "Ein- und zweidimensionale NMR-Spektroskopie: Eine Einführung", Verlag Chemie, Weinheim 1992.
[3] H. Günther, "NMR-Spektroskopie" 2. Auflage, Georg Thieme Verlag, Stuttgart 1983.
[4] T. M. Alam and G. P. Drobny, Chem. Rev. *91*, 1545 (1991).
[5] P. C. Lauterbur, Nature *242*, 190 (1973).
[6] H. Siebold and A. Ganssen, Phys. Bl. *39*, 84 (1983).
[7] H. H. Limbach, Nachr. Chem. Tech. Lab. *28*, 860 (1980).
[8] B. Boddenberg in "Lectures on Surface Science", edited by G. R. Castro and M. Cardona, Springer Verlag, Berlin 1987.
[9] B. Boddenberg and R. Grosse, Z. Naturforsch. *41a*, 1361 (1986).
[10] C. A. Fyfe, Y. Feng, H. Grondey, G. T. Kokotailo, and H. Gies, Chem. Rev. *91*, 1525 (1991).
[11] S. L. Rudaz, J.-P. Ansermet, P.-K. Wang, Ch. P. Slichter, and J. H. Sinfelt, Phys. Rev. Lett. *54*, 71 (1985).
[12] J. Klinowski, Chem. Rev. *91*, 1459 (1991).
[13] C. A. Fyfe, Y. Feng, H. Grondey, G. T. Kokotailo, and H. Gies, Chem. Rev. *91*, 1525 (1991).
[14] U. Hong, J. Kärger, B. Hunger, N. N. Feoktistova, and S. P. Zhdanov, J. Catal. *137*, 243 (1992).
[15] C. A. Fyfe, J. M. Thomas, J. Klinowski, and G. C. Gobbi, Angew. Chem. *22*, 259 (1983).
[16] C. P. Poole, "Electron Spin Resonance" Interscience Publishers, New York 1967.
[17] W. Weltner, Jr. "Magnetic Atoms and Molecules", Scientific and Academic Editions; Van Nostrand Reinhold Company, Inc., Amsterdam 1983.
[18] C. P. Keijzers, E. J. Reijerse, and J. Schmidt, "Pulsed EPR: A new field of applications", North Holland Publishers, Amsterdam 1989.

[19] S. Bagdonat, W. Göpel, and R. Haul, Z. Phys. Chem. *87*, 11 (1973).
[20] S. Bagdonat and W. Göpel, Z. Phys. Chem. *87*, 23 (1973).
[21] R. F. Howe, "Magnetic Resonance in Surface Science" in Springer Series in Chemical Physics, Vol. 35, Springer Verlag, Berlin 1984.
[22] M. Shiotani and J. H. Freed, J. Phys. Chem. *85*, 3873 (1981).
[23] M. Farle, M. Zomack, and K. Baberschke, Surf. Sci. *160*, 205 (1985).
[24] M. Zomack and K. Baberschke, Surf. Sci. *178*, 618 (1986).
[25] M. Zomack and K. Baberschke, Phys. Rev. B *36*, 5756 (1987).
[26] J. H. Freed, J. Chem. Soc. Faraday Trans. *86*, 3173 (1990).
[27] D. J. Schneider and J. H. Freed, in "Spin Labeling Theory and Applications", Vol. 8, Biological Magnetic Resonance, Press, New York (1988).
[28] J. H. Lunsford, Langmuir *5*, 12 (1989).
[29] K. Marre and H. Neddermeyer, to be published.
[30] R. M. Jaeger, H. Kuhlenbeck, H.-J. Freund, M. Wuttig, W. Hoffmann, R. Franchy, and H. Ibach, Surf. Sci. *259*, 235 (1991).
[31] M. A. van Hove, R. J. Koestner, P. C. Stair, J. P. Biberian, L. L. Kesmodel, I. Bartos, and G. A. Somorjai, Surf. Sci. *103*, 189 (1981).
[32] M. Menges, Dissertation, Ruhr-Universität Bochum, in preparation. – D. Cappus, Dissertation, Ruhr-Universität Bochum, in preparation.
[33] Th. Bertram, A. Brodde, and H. Neddermeyer, unpublished data.
[34] R. M. Jaeger, Dissertation, Ruhr-Universität Bochum, in preparation.
[35] C. F. Jackels and E. R. Davidson, J. Chem. Phys. *63*, 4672 (1975).
[36] D. S. Burch, W. H. Tanttila, and M. Mizushima, J. Chem. Phys. *61*, 1607 (1974).
[37] M. E. Bartram and B. E. Koel, Surf. Sci. *213*, 137 (1989).
[38] J. Korringa, Physica *16*, 601 (1950).
[39] T. J. Schaafsma, G. A. v. d. Velde, and J. Kommandeur, Mol. Phys. *14*, 501 (1967).
[40] T. J. Schaafsma and J. Kommandeur, Mol. Phys. *14*, 517 (1967).
[41] T. J. Schaafsma and J. Kommandeur, Mol. Phys. *14*, 525 (1967).
[42] G. R. Bird, J. C. Baird, A. W. Jache, J. A. Hodgson, R. F. Curl, A. C. Kunkle, J. W. Brandsford, J. Rastrup-Anderson, and J. Rosenthal, J. Chem. Phys. *40*, 3378 (1964).
[43] D. W. James and R. C. Marshall, J. Phys. Chem. *72*, 2963 (1968).
[44] C. A. McDowell, M. Nakajima, and P. Raghunatan, Can. J. Chem. *48*, 805 (1970).
[45] T. M. Pietrzak and D. E. Wood, J. Chem. Phys. *53*, 2454 (1970).
[46] R. D. Iyengar and V. V. Subba Rao, J. Am. Chem. Soc. *90*, 3267 (1968).
[47] J. H. Lunsford, J. Colloid Interface Sci. *26*, 355 (1968).
[48] C. Kittel and E. Abrahams, Phys. Rev. *90*, 238 (1953).
[49] M. Zomack, Dissertation, FU Berlin 1987.

Presented at the Discussion Meeting of the Deutsche Bunsen-Gesellschaft für Physikalische Chemie "In situ-Investigations of Physico-Chemical Processes at Interfaces" in Lahnstein from September 30th to October 2nd, 1992 E 8192